



Penetration, distribution, and elimination of remofuscin/soraprazan in Stargardt mouse eyes following a single intravitreal injection using pharmacokinetics and transmission electron microscopic autoradiography: Implication for the local treatment of Stargardt's disease and dry age-related macular degeneration

Sylvie Julien-Schraermeyer^{1,2}  | Barbara Illing¹ | Alexander Tschulakow^{1,2} | Tatjana Taubitz¹ | Jamil Guezzuez³ | Michael Burnet³ | Ulrich Schraermeyer^{1,2}

¹Division of Experimental Vitreoretinal Surgery, Centre for Ophthalmology, University of Tuebingen, Tübingen, Germany

²STZ Ocutox - Preclinical Drug Assessment, Hechingen, Germany

³Synovo GmbH, Tuebingen, Germany

*Correspondence

Sylvie Julien-Schraermeyer, Division of Experimental Vitreoretinal Surgery, Centre for Ophthalmology, Schleichstrasse 12/1, 72076 Tuebingen, Germany. Email: Sylvie.Julien@med.uni-tuebingen.de

Funding information

Bundesministerium für Bildung und Forschung, Grant/Award Number: 01GQ1422B

Abstract

Age-related macular degeneration (AMD) is the leading cause of blindness in older people in the developed world while Stargardt's disease (SD) is a juvenile macular degeneration and an orphan disease. Both diseases are untreatable and are marked by accumulation of lipofuscin advancing to progressive deterioration of the retinal pigment epithelium (RPE) and retina and subsequent vision loss till blindness. We discovered that a small molecule belonging to the tetrahydropyridoether class of compounds, soraprazan renamed remofuscin, is able to remove existing lipofuscin from the RPE. This study investigated the drug penetration, distribution, and elimination into the eyes of a mouse model for increased lipofuscinogenesis, following a single intravitreal injection. We measured the time course of concentrations of remofuscin in different eye tissues using high-performance liquid chromatography combined with mass spectroscopy (HPLC-MS). We also visualized the penetration and distribution of ³H-remofuscin in eye sections up to 20 weeks post-injection using transmission electron microscopic (TEM) autoradiography. The distribution of silver grains revealed that remofuscin accumulated specifically in the RPE by binding to the RPE pigments (melanin, lipofuscin and melanolipofuscin) and that it was still detected after 20 weeks. Importantly, the melanosomes in choroidal melanocytes only rarely bind remofuscin emphasizing its potential to serve as an active ingredient

Abbreviations: μ Ci, microcurie; A2E, N-retinylidene-N-retinylethanolamine; ABCA4 (previously denoted "ABCR"), ATP-binding cassette transporter; AMD, age-related macular degeneration; DMSO, dimethyl sulfoxide; ERG, electroretinogram; HPLC-MS, high-performance liquid chromatography mass spectroscopy; MALDI-IMS, matrix assisted laser desorption ionization imaging mass spectrometry; MBq, megabecquerel; PBS, Phosphate-Buffered Saline; RPE, retinal pigment epithelium; SD, Stargardt's disease; TEM, transmission electron microscopy.

This is an open access article under the terms of the Creative Commons Attribution-NonCommercial-NoDerivs License, which permits use and distribution in any medium, provided the original work is properly cited, the use is non-commercial and no modifications or adaptations are made.

© 2020 The Authors. *Pharmacology Research & Perspectives* published by British Pharmacological Society and American Society for Pharmacology and Experimental Therapeutics and John Wiley & Sons Ltd

in the RPE for the treatment of SD and dry AMD. In addition, our study highlights the importance of electron microscopic autoradiography as it is the only method able to show drug binding with a high intracellular resolution.

KEYWORDS

autoradiography, high-performance liquid chromatography mass spectroscopy, intravitreal injection, pharmacokinetic, retinal pigment epithelium, Stargardt's disease, Transmission electron microscopy

1 | INTRODUCTION

In the western world, age-related macular degeneration (AMD) is the leading cause of irreversible blindness among Caucasians over the age of 65.¹ It occurs in a wet form, with the development of abnormal blood vessels, and a dry form which accounts for about 90% of all cases. Stargardt's disease (SD) is a form of juvenile onset macular degeneration and is an orphan disease.² Dry AMD and SD are characterized by progressive loss of central vision, atrophy of the retinal pigment epithelium (RPE), and accumulation of lipofuscin.^{3,4} Both diseases result in legal blindness. Whereas, the specific pathogenic causes of AMD are multi-complex and poorly understood, SD is caused by single gene defect with either an autosomal dominant or an autosomal recessive (90%) inheritance. Loss of vision usually starts in the teenage years. The autosomal recessive form of SD is linked to mutations in the *Abca4* gene. This gene encodes an ATP-binding cassette (ABC) transport protein located in the disc membranes of rod and cone outer segments.⁵ The *Abca4* protein is involved in the transport of all-*trans*-retinal conjugates across the disc membranes. In the absence of a functional *Abca4* protein, bis-retinoid products accumulate in retinal cells, resulting in the deposition of lipofuscin, causing secondary photoreceptor degeneration.⁶ While there is no animal model for dry AMD, a pigmented *Abca4*^{-/-} mouse strain has been described and is currently used as mouse model for SD and for increased lipofuscinogenesis in general.⁷⁻¹¹

Currently, there are no Food and Drug Administration-approved treatments for SD and dry AMD, thus there is a high medical need.¹² Several small molecules have been identified for their abilities to decrease the new formation of lipofuscin in the RPE¹³⁻¹⁵; to block the formation of N-retinylidene-N-retinylethanolamine (A2E), a lipofuscin bisretinoid, from RPE¹⁶ or to remove it,¹⁷ to directly target toxic all-*trans*-retinal that forms RPE lipofuscin¹⁸ or to inhibit the formation of bisretinoids using retinol binding protein 4 antagonists.^{9,19}

We discovered that the tetrahydropyridoethers class of compounds, in particular (7R,8R,9R)-2,3-dimethyl-8-hydroxy-7-(2-methoxyethoxy)-9-phenyl-7,8,9,10-tetrahydro-5-imidazo[1,2-h][1,7]-naphthyridine (soraprazan renamed remofuscin),²⁰ a potent and reversible inhibitor of the H⁺/K⁺ ATPase, leads to a significant removal of lipofuscin from the RPE cells of healthy monkeys without obvious side-effects after a one-year oral treatment.²¹ Efficacy of remofuscin and absence of toxicity in the electroretinogram (ERG) have also been confirmed in the pigmented *Abca4*^{-/-} mice four weeks

after a single intravitreal injection as a suspension.^{22,23} Moreover the successful removal of lipofuscin from cultured primary aged human and *Abca4*^{-/-} mouse RPE cells has no cytotoxic effects and did not alter the function of RPE cells, measured by the capacity for phagocytosis.^{24,25} Therefore, remofuscin may be a promising drug candidate to manage neurodegenerative diseases related to lipofuscin accumulation. Our previous findings contributed to the Orphan Medicinal Product Designation of remofuscin for the treatment of SD in the USA and by the European Medicines Agency (EU/3/13/1208) and the funding from the European Union's Horizon 2020 research and innovation program (grant agreement No 779 317) of a proof-of-concept clinical trial for SD which is currently running under the name "STARTT: Stargardt Remofuscin® Treatment Trial: A multi-national, multi-center, double-masked, placebo-controlled proof of concept trial to evaluate the safety and efficacy of oral soraprazan in Stargardt disease" (EudraCT Number: 2018-001496-20).

In the present experimental study, the penetration, distribution, and elimination of remofuscin following a single intravitreal injection was investigated in a mouse model for SD using high-performance liquid chromatography combined with mass spectroscopy (HPLC-MS) as well as transmission electron microscopic (TEM) autoradiography and the sensitivity of both techniques was compared.

2 | MATERIALS AND METHODS

2.1 | Remofuscin and ³H-labelled remofuscin

A compound of the tetrahydropyridoethers class, Soraprazan (7R,8R,9R)-2,3-dimethyl-8-hydroxy-7-(2-methoxyethoxy)-9-phenyl-7,8,9,10-tetrahydro-5-imidazo[1,2-h][1,7]-naphthyridine) renamed remofuscin as well as the radiolabeled substance ³H-labeled remofuscin were synthesized by Chemical Lab (Tuebingen, Germany).

2.2 | Animals

Pigmented *Abca4*^{-/-} mice (129S4/SvJae-*Abca4*tm1Ght) were purchased from Charles River (Sulzfeld, Germany). This strain was bred in our in-house facility. In total 18 mice (9 females and 9 males) were used. The age of the animals was between 5 and 7 months old when starting the experiments. Light cycling was 12 hours

light (approximately 50 lux in cages)/12 hours dark, food and water were available ad libitum. All procedures involving animals were in accordance with the German laws governing the use of experimental animals and were previously approved by the local agency for animal welfare (Einrichtung für Tierschutz, Tierärztlichen Dienst und Labortierkunde der Eberhard Karls Universität Tübingen, Germany) and the local authorities (Regierungspräsidium Tübingen, Germany).

2.3 | Pharmacokinetic study

A suspension of 40 µg of remofuscin in 2 µL of PBS containing 1% DMSO was intravitreally injected in both eyes of seven pigmented *Abca4*^{-/-} mice (three females and four males), one untreated mouse (a female) served as control. After euthanasia, the eyes were immediately enucleated and stored in PBS at +4°C overnight for a better separation of the retina from the RPE/choroid complex. The next day, the eyes were prepared in two parts, cornea, iris, ciliary body, lens, vitreous and retina separated from the RPE, choroid and sclera. The samples were weighed and stored at -80°C until further processing. Remofuscin was quantified before injection (control), 2 hours, 1, 3, 7, 14, 21, and 28 days after injection. Two eyes per time point were investigated and statistically analyzed using Microsoft excel to calculate mean. No formal hypothesis or comparison was made or tested, however, mean values were used to model standard pharmacokinetic parameters of Area under the concentration/ time curve (AUC) and half-life in the eye. To this end, the PKF Exel Macros were employed (Joel I. Usansky, PhD, Atul Desai, MS and Diane Tang-Liu, PhD Department of Pharmacokinetics and Drug Metabolism Allergan, Irvine, CA 92606, USA).

2.4 | HPLC-MS

A liquid chromatography–electrospray ionization–tandem mass spectrometry (LC–ESI–MS–MS) method was developed for determination of remofuscin in mouse eyes. Each eye was divided into an anterior (cornea, retina, iris and vitreous) and a posterior (sclera, chorioidea and RPE) compartment. Samples were weighed, and homogenized in 6 volumes (6 µL of solvent per mg tissue) of acetonitrile containing 10 nM internal standard, and after centrifugation (14 000 g, 5 min) the supernatant was prepared for analysis by LC–ESI–MS–MS system. Chromatographic separation used a C18 (Reposil-pur column, 60 × 2 mm, 3 µm, Dr Maisch, Ammerbuch, Germany) using an Agilent 1260 HPLC with column maintained at 45°C. The mobile phases were water (A) and acetonitrile:water (B) (90:10, v/v) containing 0.1% formic acid, at a flow rate of 0.5 mL/min. The injected sample volume was 6 µL which was eluted using the following gradient, 0 - 0.5 min, 10% B; 2-5 min, 100% B; and 6-9 min, 10% B to allow column re-equilibration. Mass-spectrometric quantification was

performed on API 4000 Triple Quad mass spectrometer using Analyst 1.6.2 for data acquisition (Applied Biosystems Sciex), in the multiple reaction monitoring (MRM) mode. Remofuscin was detected with the m/z transition 368.1 → 292.2 in positive ion mode. The linear calibration curve covered a concentration range of 5-100000 nmol/L. Remofuscin standard (10 mmol/L) was prepared in DMSO, and further diluted with water/acetonitrile to obtain the calibration samples. Quality control (QC) samples of 1000 nM were prepared in a similar manner. A comparison to a linear regression of the standard curve was used to calculate sample concentrations. Results were calculated in nmol/kg tissue weight.

2.5 | ³H-Labelled remofuscin dosing and endpoints

Both eyes of 10 pigmented *Abca4*^{-/-} mice (5 females and 5 males) were intravitreally injected with two µL of a suspension of ³H-labelled remofuscin. The radiolabeled substance was suspended extemporaneously in PBS containing 1% DMSO on the day of injection. The target dose level was about 40 µg/eye, and the radioactive dose approximately 4 MBq (104 µCi)/ eye.

Nine endpoints were defined and two eyes per time points were investigated. The mice were sacrificed 2 hours (h), 1 day (d), 1 week (w), 2 w, 4 w, 6 w, 8 w, 12 w, and 20 w post-dose.

2.6 | Intravitreal injection

The mice were anaesthetized with an intraperitoneal injection of a three-component narcosis (0.05 mg fentanyl, 5.00 mg midazolam and 0.5 mg of medetomidine/1 kg body weight). The reagents were purchased from Albrecht GmbH, Aulendorf; Hameln Pharma Plus GmbH, Hameln and Alfavet, Neumuenster in Germany. The pupils were dilated with 1 to 2 drops of Mediatricum drops (Pharmacy of the University of Tuebingen, Germany) and a drop of topical anesthetic Novesine (OmniVision, Puchheim, Germany) was applied. Methocel (OmniVision, Puchheim, Germany) eye drops were used to avoid drying of the eyes. Injections were performed using a surgical microscope equipped with illumination. A small incision was made into the conjunctiva at the outer corner of the eyes. The eyeball was rotated by grasping the conjunctiva with a pair of fine tweezers and gentle pulling. A volume of 2 µL was injected through the hole intravitreally using a 10 µL NanoFil syringe with a NanoFil 34 gauge beveled needle (World Precision Instruments). After the injection, the needle remained in the eye for an additional 3 or 4 seconds to reduce reflux and was then drawn back. The eyeball was brought back into its normal position, and the antibiotic ointment was applied to the eye (Gentamicin-POS®, Ursapharm, Saarbruecken, Germany). Finally, the mice were injected s.c. with an antidote (1.2 mg naloxon, 0.5 mg flumazenil, 2.5 mg atipamezol/1 kg body weight) which neutralized the anesthetic. The reagents were purchased from Hameln Pharma

Plus GmbH, Hameln; Fresenius-Kabi, Bad Homburg and Alfavet, Neumuenster in Germany.

2.7 | Sample preparation and transmission electron microscopic (TEM) autoradiography

Animals were sacrificed by carbon dioxide inhalation and subsequent cervical dislocation and the eyes were immediately enucleated.

For electron microscopy, eyes were fixed overnight at 4°C in 5% glutaraldehyde in 0.1 M cacodylate buffer (pH 7.4). After washing in cacodylate buffer, the cornea and lens were removed. The eye cups were then post-fixed with 1% osmium tetroxide in 0.1 M cacodylate buffer for 2 hours, dehydration was then started by a series of incubations in 30%, 50%, 70%, 80%, 96% and absolute ethanol. The samples were then embedded in Epon. Reagents were purchased from AppliChem (Darmstadt, Germany), Merck (Darmstadt, Germany), and Serva (Heidelberg, Germany). Ultrathin sections (80 nm) were cut with an ultra-microtome (Ultracut E, Reichert) and mounted to polylysine coated nickel grids (100 mesh, hexagonal).

All further autoradiography-implementations were performed in a darkroom illuminated with green light. For nuclear emulsion the Ilford Emulsion L4 was used. The solution was made up extemporaneously, melted in a glass vessel in a water bath at 40°C. To ensure an even, uniform and thin layer of emulsion, the heated emulsion was diluted 1 + 7 with deionized water. A platinum wire loop was dipped into the emulsion in order to form a thin, even membrane which was applied to the specimen by touching.

After coating and drying the grids in the darkroom at room temperature for 1h, emulsion coated sections were stored for the exposure period in light sealed boxes with silica gel orange at 4°C. Specimens were exposed between 10 to 20 days and afterwards developed with Kodak GBX developer for 3 minutes, washed with deionized water, fixed for 3 minutes with Ilford Ilfostop and washed again. Post-staining with lead citrate was performed for 1 minute from the non-coated side of the grid. After drying sections were observed and analyzed under an electron microscope (model 900; Carl Zeiss, Jena, Germany).

2.8 | Quantification of ³H-remofuscin binding to melanin, lipofuscin and melanolipofuscin in RPE

Autoradiographed sections of *Abca4*^{-/-} mouse eyes were comprehensively examined by electron microscopy (Zeiss TEM 900). To determine the distribution and the dwell time of remofuscin in the tissue, nine different time-points were investigated after a single intravitreal injection of ³H-remofuscin (2 hours, 1 day, 1, 2, 4, 6, 8, 12, and 20 weeks after injection). For each time point 1-2 eyes were reviewed. To statistically analyze the binding specificity of remofuscin to RPE pigments, electron micrographs of comparable

sections of the RPE (12.000 x magnification) were taken (4-40 digital images per section).

The number of silver grains was counted within the cytoplasm of RPE cells at a length of 10 μm RPE in each micrograph and analyzed statistically using an ANOVA with Tukey post hoc test.

3 | RESULTS

3.1 | Pharmacokinetics of remofuscin in eyes after a single intravitreal injection in pigmented *Abca4*^{-/-} mice

Following intravitreal injection, remofuscin was recovered from both the front and back of the eye. The relative amounts initially favored the front components, however, over time, the differential decreased. The initial higher concentrations in the front of the eye may reflect transport of remofuscin in aqueous flow from the back to the front of the eye. The reduction of this differential over time is likely due to the affinity of remofuscin for the lipophilic components of the RPE while having no specific binding sites in the front of the eye. Following application, the initial half-life was approximately 12 hours. However, following absorption to the RPE, the terminal half-life of remofuscin in the RPE in the mouse approximates to a week (5,8 days in the anterior compartment, and 6.1 days in the posterior compartment).

The amount of remofuscin decreased with time but remained in the vitreous and in the RPE four weeks after injection (Figure 1). The bulk concentration in the anterior compartment was 490 nmol/kg (approximates to nM) and 154 nmol/kg in the posterior compartment at day 28. The area under the time concentration curve was 78 μmol/kg*d for the anterior compartment and 27 μmol/kg*d for the posterior compartment which likely reflects clearance to the front of the eye by aqueous flow.

3.2 | Distribution of radioactivity using transmission electron microscopic autoradiography

The distribution of radioactivity (silver grains) in the posterior pole of the eye of pigmented *Abca4*^{-/-} mice following a single intravitreal injection of ³H-remofuscin was determined in a subjective manner using TEM autoradiography. Since the mode of action of remofuscin is to remove mainly lipofuscin and melanolipofuscin from the RPE,²¹ only tissues of the posterior pole of the eye were selected for analysis and are presented in Table 1 and illustrated in Figure 2. The quantification of silver grains per 10 μm RPE length is shown in Figure 3. The highest distribution of silver grains was observed in the RPE at all sampling time starting 2 hours post-injection until 20 weeks after injection of ³H-remofuscin. Occasionally, low level or only traces of silver grains were also detected in the retina, the Bruch's membrane and the choroid.

FIGURE 1 Concentration vs time following intravitreal application of 40 µg remofuscin/eye. The two data points are shown for each time point (n = 2 eyes/time point). The X-axis indicates the time in day, the Y-axis shows the concentration of remofuscin in nmol/kg. Anterior compartment: cornea, iris, ciliary body, lens, vitreous, and retina. Posterior compartment: RPE, choroid, and sclera

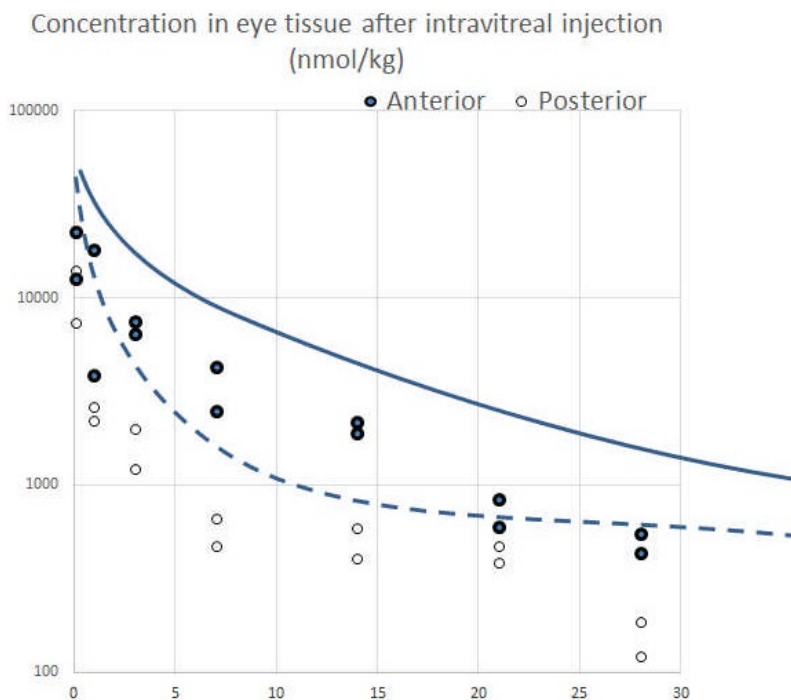


TABLE 1 Qualitative assessment of radioactivity in the posterior pole of the eye of pigmented *Abca4*^{-/-} mice after a single intravitreal injection of ³H-remofuscin

Tissue Sampling time	2hrs	d1	w1	w2	w4	w6	w8	w12	w20
Retina	++	+	-	-	-	-	-	-	-
RPE	+	++++	++++	+++	+++	++	++	++	++
Bruch's membrane	++	+	-	-	-	-	-	-	-
Choroid: red blood cells	++	+	†	-	-	-	-	-	-
Choroid: melanocytes	-	†	†	†	†	-	-	-	-

Note: ++++ Very high levels of silver grains; +++ high levels of silver grains; ++ moderate levels of silver grains; + low levels of silver grains; † trace of silver grains, - no silver grains (hrs, hours; d, day; w, week).

3.3 | Quantification of radioactivity in the RPE using transmission electron microscopic autoradiography

The amount of silver grains within the cytoplasm of RPE cells at a length of 10 µm RPE was determined at all nine time points following a single intravitreal injection of ³H-remofuscin in pigmented *Abca4*^{-/-} mice.

Given that little or no metabolism of remofuscin has been observed in the eye, and there is no loss of ³H via exchange to solvent, the presence of silver grains indicated the presence of radioactive labeled remofuscin. These grains were found at all investigated time points with a peak between day 1 (14 ± 3.5) and day 7 (14.9 ± 7.5) after the administration. Between week 1 (14.9 ± 7.5) and week 2 (5 ± 8.7), the amount of silver grains decreases considerably. After week 4 (6.6 ± 4.6), it decreases slowly. Noticeably, the silver grains were still detectable 20 weeks (2.2 ± 3.8) after a single intravitreal injection of ³H-remofuscin (Figure 3).

4 | DISCUSSION

Pathogenic events in SD and dry AMD are very similar. In both diseases, the accumulation of lipofuscin in cells of the RPE is a hallmark of the disease.²⁶ Lipofuscin is regarded as a waste product which accumulates in post-mitotic cells in the body and it can occupy a considerable portion of the free cytoplasmic space of RPE cells. Lipofuscin and one of its components, A2E, have been shown to exert a number of negative effects for the retina.²⁷ It is stored in storage compartments called lysosomes. In cells unable to divide, such as RPE cells, it is accumulated over a life time. The continuous accumulation over time has been recognized for more than 100 years, but the exact mechanisms behind lipofuscin accumulation are still unclear.

In patients with advanced dry AMD, retinal areas adjacent to geographic atrophy that have the highest accumulation of lipofuscin were the area most likely to lose function in subsequent years.^{28,29} Although lipofuscin composition varies between different types of

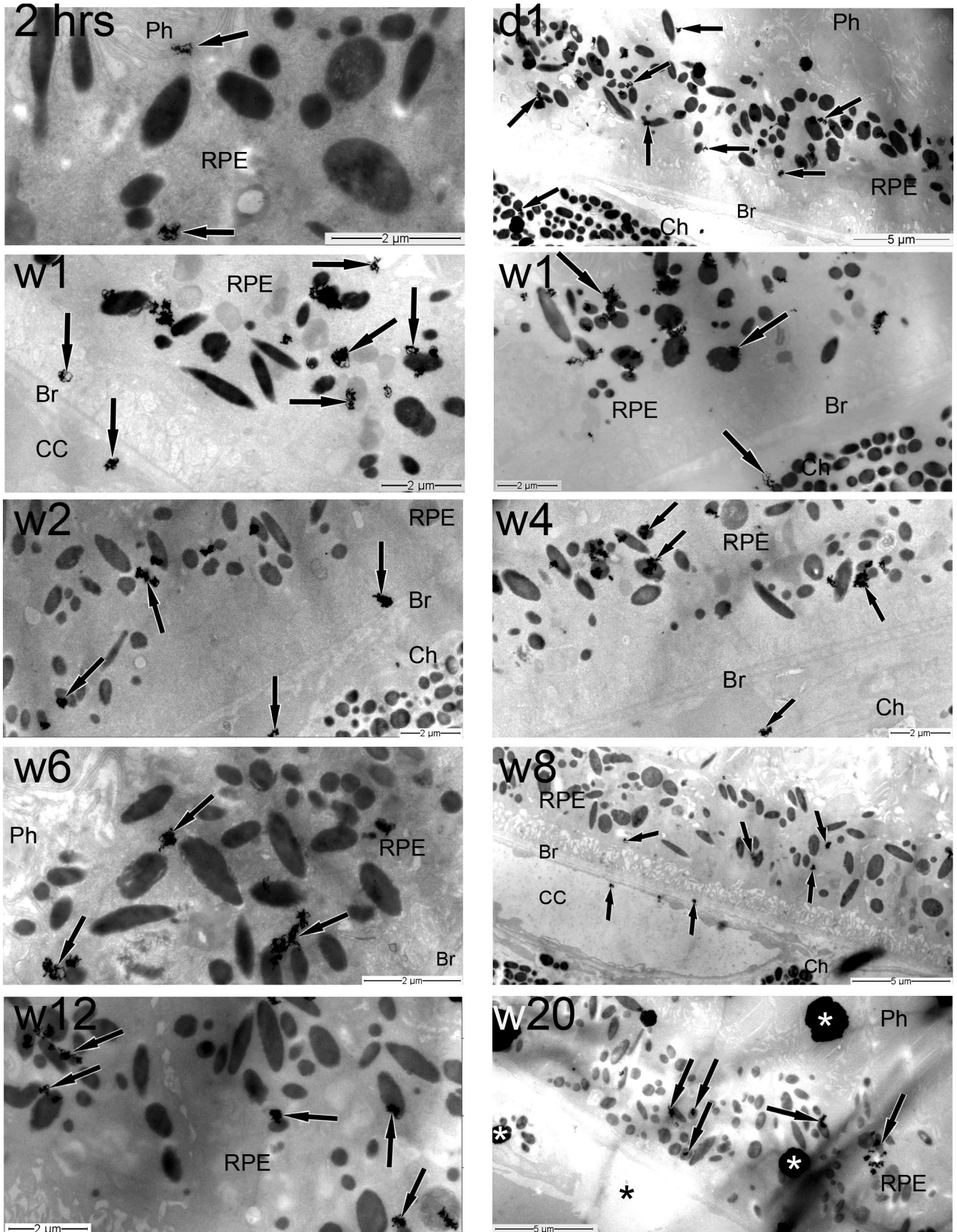


FIGURE 2 Time course TEM autoradiographic distribution of ^3H -remufusin (indicated by the presence of silver grains) in the posterior pole of the eye following a single intravitreal administration. The magnification calibration in micrometers is indicated in each electron micrograph. The black arrows show the silver grains, the asterisks indicate artefacts. Br, Bruch's membrane; CC, choriocapillaris; Ch, choroid; d, day; hrs, hours; Ph, photoreceptors; RPE, retinal pigment epithelium; w, week

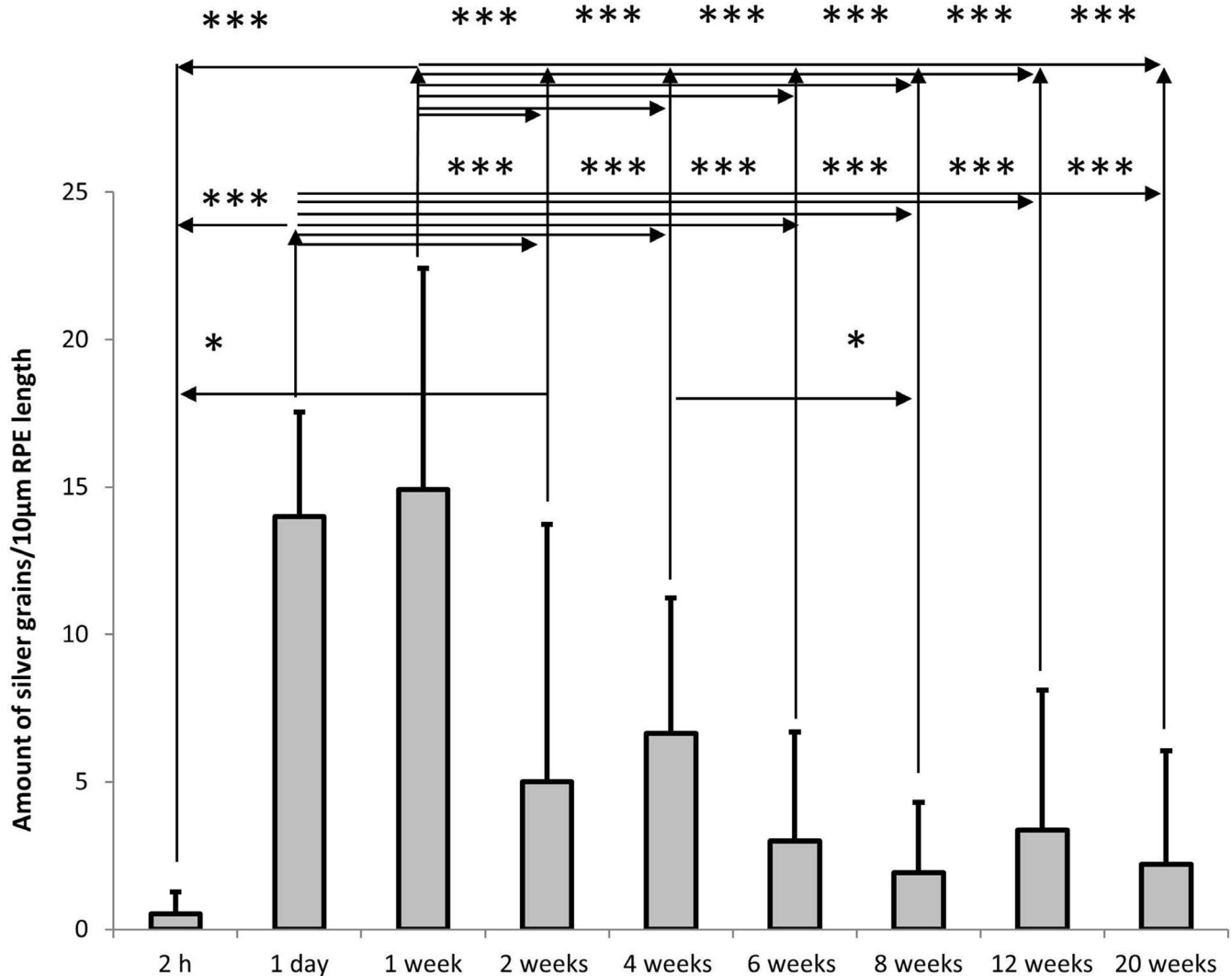


FIGURE 3 Time course quantification of silver grains within the cytoplasm of RPE cells at a length of 10 μm indicating the amount of radioactive labeled remofuscin in the RPE of pigmented *Abca4*^{-/-} mice, shown as mean and standard deviation plots. Electron micrographs (4-40 digital images per section) of comparable sections of the RPE (12,000 x magnification) were taken. The results of an ANOVA analysis with Tukey post hoc test are shown: * for $P < .05$, *** for $P < .0001$

cells that suffer from its accumulation, all lipofuscin pigments were always reported to be non-degradable.³⁰ It was then notable and surprising that lipofuscin could be removed from RPE cells of monkeys after oral treatment with remofuscin.²¹ The proof of concept was also demonstrated in aged human and mouse cultured RPE cells^{24,25} as well as in the SD mouse model after a single intravitreal injection of remofuscin.^{22,23} Unlike existing approaches targeting lipofuscin formation process such as Alkeus Pharmaceuticals' oral substance ALK-001 (C20-D3-retinyl acetate) already in clinical phase 2, remofuscin reduces existing levels of lipofuscin in the RPE instead of merely slowing down accumulation of further toxic Vitamin A aggregates.¹² The effect of oral administered remofuscin is currently under investigation in a proof of concept clinical study in Stargardt's disease patients.

Intravitreal injections of drug suspensions are being increasingly employed in the delivery of drugs to the posterior segment diseases where the target site is the macular region³¹ and are

well tolerated by patients. Since SD patients are generally young patients, a drug that only needs to be intravitreally injected infrequently will be of great value. Therefore, the penetration, distribution and the duration of accumulation of remofuscin was investigated in this study. To obtain valid pre-clinical data, pigmented *Abca4*^{-/-} mice were used since it is the only animal model that reflects the melanin and (melano)- lipofuscin pigmentation similar to SD and dry AMD patients.¹⁰ Importantly, many studies have investigated the binding between drugs and melanin^{31,32} but our study is the first reporting in addition, the binding between a drug and melanolipofuscin and lipofuscin, two pigments present in high amounts in the elderly population and in patients suffering from SD and dry AMD.

Although TEM autoradiography is a laborious technique, it was chosen because it is the only method that is able to show precisely where the drug is located. Using ³H, this approach yields high cellular and subcellular resolution (about 160 nm).³³ In comparison, the

spatial resolution of matrix assisted laser desorption ionization imaging mass spectrometry (MALDI IMS) is now only capable of uniting low micrometer spatial resolution allowing to differentiate the RPE and the photoreceptor layers^{34,35} but not to distinguish the different granules within the RPE.

In contrast to autoradiography, LC-MSMS has less spatial resolution but is more able to identify the molecular species involved (radioactivity can also be derived from metabolites of the parent material administered). The objective of determining the local pharmacokinetics via LCMS was to confirm both that remofuscin was present in its unmetabolized form, and to determine the likely bulk tissue distribution. The tissues studied essentially consist of the front and back of the eye. The back of the eye is dominated by the RPE in which hydrophobicity due to lipid, retinoid and melanin species leads to considerable drug absorption. The front of the eye is not considered the specific target of this therapy and tends to have more hydrophilic surfaces. The kinetics following intravitreal application consists of two opposing actions: absorption to tissue via hydrophobic and electrostatic interactions, and transport in the aqueous flow to the front of the eye. The drug is deposited as a fine suspension in the narrow space between the lens and the retina. The suspended material and associated soluble material then partitions between the aqueous and the solid components in the eye driven largely by differential solubility in the aqueous and membrane compartments. The RPE in particular acts as a sink allowing further dissolution and diffusion of remofuscin to the back of the eye where it is partitioned onto lipophilic sites by equilibrium. Remofuscin has a nominal solubility maximum in vitreous/water of circa 1 $\mu\text{mol/L}$ based on our assays. The aqueous is exchanged up to 6 times per day thus, there is a constant aqueous elimination process dissolving and transporting the drug away. The kinetics that we observed are consistent with this general model of a depot reaching the RPE and being slowly exchanged by diffusion to the aqueous flow over a period of up to 4 weeks. The loss to aqueous is dominated by the partition coefficient for remofuscin (LogP 3-4) which favors solubility in lipid environments such as the RPE.

This study highlighted a depot effect of remofuscin in the RPE (Table 1, Figure 3) likely due to its ability to bind specifically RPE pigments. Indeed, it was shown that melanin binding affects the distribution and elimination of ocular drugs and that drugs administered intravitreally reach much higher concentrations in ocular tissues than systemically administered drugs and their accumulation into the pigmented tissues is greater.³² In rare instances, binding between remofuscin and choroidal melanocytes was observed by autoradiography. This can be due to chemical differences between melanosomes of RPE and choroidal melanocytes³⁶ or due to the filter property of the RPE³⁷ and/or the elimination of remofuscin *via* the choriocapillaris inhibiting the further penetration into the choroid. Consistent with this, studies in rats indicated that remofuscin binds specifically to pigments of the RPE after oral application (data not shown).

It is known that many substances, even when administered systematically for non-ocular pathologies (eg, hydroxychloroquine), may induce ocular toxicological complications leading to retinal degeneration due to their affinity to melanin.³⁸ Although remofuscin clearly showed affinity to RPE pigments (Figure 2), neither a one-year oral treatment in monkeys²¹ nor a single intravitreal injection^{22,23} induced ocular side-effects as monitored by ERG. The fact that remofuscin not only associates with lipofuscin but also with melanolipofuscin and melanin could be an advantage for the treatment of dry AMD or SD patients since it has been shown that these two pigments are associated with toxicity with increasing age³⁹ or during disease.⁴⁰ In the current study, the removal of pigments induced by remofuscin treatment was not investigated therefore it is not excluded that at least a part of the diminution of silver grain amounts over time may be due to the elimination of the pigments bound to remofuscin.

To conclude, this study confirms the specific affinity of remofuscin to pigments of the RPE in an animal disease model. Twenty weeks after a single injection of remofuscin, traces of the drug were still detected in the RPE showing a depot effect. However, attention should be taken since these findings were obtained in a mouse disease model and they may be not extrapolated completely to normal mouse strain or to human tissue. Indeed, previous studies reported about chemical and ultrastructural variations of lipofuscin and melanolipofuscin in different mouse strains^{10,41} as well as variation in melanin content between different species and even between regions of the same tissue.³¹

Moreover this study emphasizes the importance of TEM autoradiography which is the only method that can show drug binding with high intracellular resolution of about 0.1 micron for tritium.⁴²

ACKNOWLEDGEMENTS

The authors thank Sigrid Schultheiss (Division of Experimental Vitreoretinal Surgery, Centre for Ophthalmology, University of Tuebingen, Germany) for her excellent technical assistance. This work was supported by "Bundesministerium für Bildung und Forschung", Bonn, Germany (Grant 01GQ1422B).

DISCLOSURE

SJS, MB, and US are founders of Katairo GmbH. JG is employee of Synovo GmbH, MB is managing director of Synovo GmbH.


AUTHOR CONTRIBUTIONS

SJS and US participated in research design. SJS, BI, AT, and JG conducted experiments. SJS, BI, AT, TT, JG, MB, and US performed data analysis. SJS, BI, and MB wrote or contributed to the writing of the manuscript. SJS and MB contributed to revision of the manuscript. All authors contributed to and have approved the final manuscript.

DATA AVAILABILITY STATEMENT

The data that support the findings of this study are available from the corresponding author upon reasonable request.

ORCID

Sylvie Julien-Schraermayer  <https://orcid.org/0000-0002-2322-511X>

REFERENCES

- Pauleikhoff D, Holz FG. Age-related macular degeneration. 1. Epidemiology, pathogenesis and differential diagnosis. *Ophthalmologe*. 1996;93(3):299-315.
- North V, Gelman R, Tsang SH. Juvenile-onset macular degeneration and allied disorders. *Dev Ophthalmol*. 2014;53:44-52.
- Vasireddy V, Wong P, Ayyagari R. Genetics and molecular pathology of Stargardt-like macular degeneration. *Prog Retin Eye Res*. 2010;29(3):191-207.
- Wolf G. Lipofuscin and macular degeneration. *Nutr Rev*. 2003;61(10):342-346.
- Molday RS, Zhang K. Defective lipid transport and biosynthesis in recessive and dominant Stargardt macular degeneration. *Prog Lipid Res*. 2010;49(4):476-492.
- Tsybovsky Y, Molday RS, Palczewski K. The ATP-binding cassette transporter ABCA4: structural and functional properties and role in retinal disease. *Adv Exp Med Biol*. 2010;703:105-125.
- Weng J, Mata NL, Azarian SM, Tzekov RT, Birch DG, Travis GH. Insights into the function of Rim protein in photoreceptors and etiology of Stargardt's disease from the phenotype in abcr knockout mice. *Cell*. 1999;98(1):13-23.
- Mata NL, Tzekov RT, Liu X, Weng J, Birch DG, Travis GH. Delayed dark-adaptation and lipofuscin accumulation in abcr^{+/−} mice: implications for involvement of ABCR in age-related macular degeneration. *Invest Ophthalmol Vis Sci*. 2001;42(8):1685-1690.
- Racz B, Varadi A, Kong J, et al. A non-retinoid antagonist of retinol-binding protein 4 rescues phenotype in a model of Stargardt disease without inhibiting the visual cycle. *J Biol Chem*. 2018;293(29):11574-11588.
- Taubitz T, Tschulakow AV, Tikhonovich M, et al. Ultrastructural alterations in the retinal pigment epithelium and photoreceptors of a Stargardt patient and three Stargardt mouse models: indication for the central role of RPE melanin in oxidative stress. *PeerJ*. 2018;6:e5215.
- Charbel Issa P, Barnard AR, Singh MS, et al. Fundus autofluorescence in the Abca4^(−/−) mouse model of Stargardt disease—correlation with accumulation of A2E, retinal function, and histology. *Invest Ophthalmol Vis Sci*. 2013;54(8):5602-5612.
- Sears AE, Bernstein PS, Cideciyan AV, et al. Towards Treatment of Stargardt Disease: Workshop Organized and Sponsored by the Foundation Fighting Blindness. *Transl Vis Sci Technol*. 2017;6(5):6.
- Charbel Issa P, Barnard AR, Herrmann P, Washington I, MacLaren RE. Rescue of the Stargardt phenotype in Abca4 knockout mice through inhibition of vitamin A dimerization. *Proc Natl Acad Sci U S A*. 2015;112(27):8415-8420.
- Maiti P, Kong J, Kim SR, Sparrow JR, Allikmets R, Rando RR. Small molecule RPE65 antagonists limit the visual cycle and prevent lipofuscin formation. *Biochemistry*. 2006;45(3):852-860.
- Radu RA, Han Y, Bui TV, et al. Reductions in serum vitamin A arrest accumulation of toxic retinal fluorophores: a potential therapy for treatment of lipofuscin-based retinal diseases. *Invest Ophthalmol Vis Sci*. 2005;46(12):4393-4401.
- Radu RA, Mata NL, Nusinowitz S, Liu X, Sieving PA, Travis GH. Treatment with isotretinoin inhibits lipofuscin accumulation in a mouse model of recessive Stargardt's macular degeneration. *Proc Natl Acad Sci U S A*. 2003;100(8):4742-4747.
- Nociari MM, Lehmann GL, Perez Bay AE, et al. Beta cyclodextrins bind, stabilize, and remove lipofuscin bisretinoids from retinal pigment epithelium. *Proc Natl Acad Sci U S A*. 2014;111(14):E1402-1408.
- Maeda A, Golczak M, Chen Y, et al. Primary amines protect against retinal degeneration in mouse models of retinopathies. *Nat Chem Biol*. 2011;8(2):170-178.
- Dobri N, Qin Q, Kong J, et al. A1120, a nonretinoid RBP4 antagonist, inhibits formation of cytotoxic bisretinoids in the animal model of enhanced retinal lipofuscinogenesis. *Invest Ophthalmol Vis Sci*. 2013;54(1):85-95.
- Simon WA, Herrmann M, Klein T, et al. Soraprazan: setting new standards in inhibition of gastric acid secretion. *J Pharmacol Exp Ther*. 2007;321(3):866-874.
- Julien S, Schraermayer U. Lipofuscin can be eliminated from the retinal pigment epithelium of monkeys. *Neurobiol Aging*. 2012;33(10):2390-2397.
- Taubitz T, Peters T, Pöschel S, et al. Removal of lipofuscin from the RPE of Abca4^{−/−} mice with THPE: quantitative and toxicity studies. *Invest Ophthalmol Vis Sci*. 2015;56(7):4199-4199.
- Fang Y, Tschulakow A, Tikhonovich M, et al. Preclinical results of a new pharmacological therapy approach for Stargardt disease and dry age-related macular degeneration. *Invest Ophthalmol Vis Sci*. 2017;58(8):256-256.
- Julien S, Biesemeier A, Heiduschka P, et al. Lipofuscin can be eliminated from retinal pigment epithelium after drug treatment. *Invest Ophthalmol Vis Sci*. 2010;51(13):481-481.
- Taubitz T, Fang Y, Rittgarn M, Schraermayer U, Julien-Schraermayer S. Testing a new pharmacological therapy approach for the removal of lipofuscin in vitro: results from a newly established culture of aged primary Stargardt mouse model RPE cells and aged primary human RPE cells. *Invest Ophthalmol Vis Sci*. 2017;58(8):257-257.
- Sparrow JR, Boulton M. RPE lipofuscin and its role in retinal pathology. *Exp Eye Res*. 2005;80(5):595-606.
- Brunk UT, Terman A. Lipofuscin: mechanisms of age-related accumulation and influence on cell function. *Free Radic Biol Med*. 2002;33(5):611-619.
- Schmitz-Valckenberg S, Fleckenstein M, Scholl HP, Holz FG. Fundus autofluorescence and progression of age-related macular degeneration. *Surv Ophthalmol*. 2009;54(1):96-117.
- Holz FG, Bindewald-Wittich A, Fleckenstein M, Dreyhaupt J, Scholl HP, Schmitz-Valckenberg S, Group FA-S. Progression of geographic atrophy and impact of fundus autofluorescence patterns in age-related macular degeneration. *Am J Ophthalmol*. 2007;143(3):463-472.
- Terman A, Brunk UT. Lipofuscin. *Int J Biochem Cell Biol*. 2004;36(8):1400-1404.
- Durairaj C, Chastain JE, Kompella UB. Intraocular distribution of melanin in human, monkey, rabbit, minipig and dog eyes. *Exp Eye Res*. 2012;98:23-27.
- Rimpela AK, Schmitt M, Latonen S, et al. Drug distribution to retinal pigment epithelium: studies on melanin binding, cellular kinetics, and single photon emission computed tomography/computed tomography imaging. *Mol Pharm*. 2016;13(9):2977-2986.
- Plattner H, Zingsheim H-P. Elektronenmikroskopische Methodik in der Zell- und Molekularbiologie ein kritischer Leitfaden zur biologischen Ultrastrukturforschung für Biologen und Mediziner; 23 Tabellen. Stuttgart [u.a.]: Fischer. 1987.
- Anderson DMG, Ablonczy Z, Koutalos Y, et al. Bis(monoacylglycerol) phosphate lipids in the retinal pigment epithelium implicate lysosomal/endosomal dysfunction in a model of Stargardt disease and human retinas. *Sci Rep*. 2017;7(1):17352.
- Anderson DMG, Messinger JD, Patterson NH, et al. Lipid landscape of the human retina and supporting tissues revealed by high-resolution imaging mass spectrometry. *J Am Soc Mass Spectrom*. 2020.
- Schraermayer U, Heimann K. Current understanding on the role of retinal pigment epithelium and its pigmentation. *Pigment Cell Res*. 1999;12(4):219-236.
- Strauss O. The retinal pigment epithelium in visual function. *Physiol Rev*. 2005;85(3):845-881.

38. Mecklenburg L, Schraermeyer U. An overview on the toxic morphological changes in the retinal pigment epithelium after systemic compound administration. *Toxicol Pathol.* 2007;35(2):252-267.
39. Rozanowski B, Burke J, Sarna T, Rozanowska M. The pro-oxidant effects of interactions of ascorbate with photoexcited melanin fade away with aging of the retina. *Photochem Photobiol.* 2008;84(3):658-670.
40. Cideciyan AV, Swider M, Schwartz SB, Stone EM, Jacobson SG. Predicting progression of ABCA4-associated retinal degenerations based on longitudinal measurements of the leading disease front. *Invest Ophthalmol Vis Sci.* 2015;56(10):5946-5955.
41. Radu RA, Mata NL, Bagla A, Travis GH. Light exposure stimulates formation of A2E oxiranes in a mouse model of Stargardt's macular degeneration. *Proc Natl Acad Sci USA.* 2004;101(16):5928-5933.
42. Caro LG, Schnos M. Tritium and phosphorus-32 in high-resolution autoradiography. *Science.* 1965;149(3679):60-62.

How to cite this article: Julien-Schraermeyer S, Illing B, Tschulakow A, et al. Penetration, distribution, and elimination of remofuscin/soraprazan in Stargardt mouse eyes following a single intravitreal injection using pharmacokinetics and transmission electron microscopic autoradiography: Implication for the local treatment of Stargardt's disease and dry age-related macular degeneration. *Pharmacol Res Perspect.* 2020;00:e683. <https://doi.org/10.1002/prp2.683>